Available online at www.sciencedirect.com
SCIENCE DIRECT
Polymer 46 (2005) 7028–7036
polymer
www.elsevier.com/locate/polymer

Intensive electric arc interaction with polymer surfaces: reorganization of surface morphology and microstructure

S. Markutsya[a], M. Rapeaux[b,**], V.V. Tsukruk[a,*]

[a]*Materials Science and Engineering Department, Iowa State University, 3155 Gilman, Ames, IA 50011, USA*
[b]*Square D/Schneider Electric, Cedar Rapids, IA, USA*

Received 6 January 2005; received in revised form 22 May 2005; accepted 24 May 2005
Available online 6 July 2005

Abstract

Intense electrical arcs were applied to thermoplastic (polyamide 66) and thermoset (fiber reinforced laminated polyester) materials and the resulting carbonization/metallization process was studied on a sub-micron scale with atomic force microscopy to understand very initial stage of reorganization of surface morphology. These changes can be critical in dramatic changes in surface resistivity preceding electric breakthrough. The surface microroughness and the localization of micro- and nanoparticles at the center (arc initiation area) and along the edges of the samples were significantly different for different arc regimes. We suggested that for thermoset, the material is pulled out of the surface in the arc formation area (the center of sample). Afterwards, the intensive re-deposition occurred along the edges enhancing non-uniform ablation around the arc initiation area. In contrary, for thermoplastic samples, the entire polymer surface was re-melted that resulted in dramatic smoothing of the initially non-uniform surface morphology.

Keywords: Electric arc; Plastic surfaces; AFM

1. Introduction

In the event of a short-circuit in a powerful circuit breaker the intense electric arc is formed with the local temperature instantly soaring up to 20,000 °C initiating active plasma in the vicinity of metal contacts and a plastic substrate [1,2]. After the arc extinguishes, the airborne metal/soot mixture formed in the vicinity of the arc initiation condenses onto surrounding insulating surfaces of the arc chamber within the circuit breaker. Such a condensation may lead to current leak or even dielectric breakdown under certain conditions [3,4]. It is believed that the atomic composition of these deposits depends on the arc energy and gas and electrode compositions for a particular circuit breaker design [5]. The type of plastic material used in the arc chambers affects significantly a sequence of events and studies were conducted to find materials with best resistance to arc exposure, good dielectric recovery, and acceptable post-arc voltage characteristics [6,7].

The surface morphology of plastic materials after the interaction with arc shots changes significantly due to intensive interaction with plasma followed by soot condensation as was discussed in several publications [5,7]. Information about the surface morphology of the affected substrates in a micron range and at larger scales is generally obtained by using optical microscopy or scanning electron microscopy (SEM), e.g. SEM data for plastics exposed to electrical arc usually demonstrates very corrugated surface morphology with a thick layer of non-uniform metal–carbon deposits and exposed glass fibers for the fiber-reinforce plastic composites (Fig. 1 for an example of surface morphology at $300\times300\ \mu m^2$). From SEM analysis it is also possible to get qualitative surface distribution of elements from large deposits. Spectroscopic analysis shows significant presence of metal from electrodes within large flakes and agglomerates along with carbonized material [8].

However, modest resolution of such techniques prevents addressing the question of the very initial stage of the surface deposit formation. Surface reorganization can occur on a sub-micron scale predominantly at earlier stages of

* Corresponding authors. Tel.: +1 515 294 6904; fax: +1 515 294 5444.
E-mail addresses: michel.rapeaux@fr.schneiderelectric.com (M. Rapeaux), vladimir@iastate.edu (V.V. Tsukruk).

0032-3861/$ - see front matter © 2005 Elsevier Ltd. All rights reserved.
doi:10.1016/j.polymer.2005.05.110

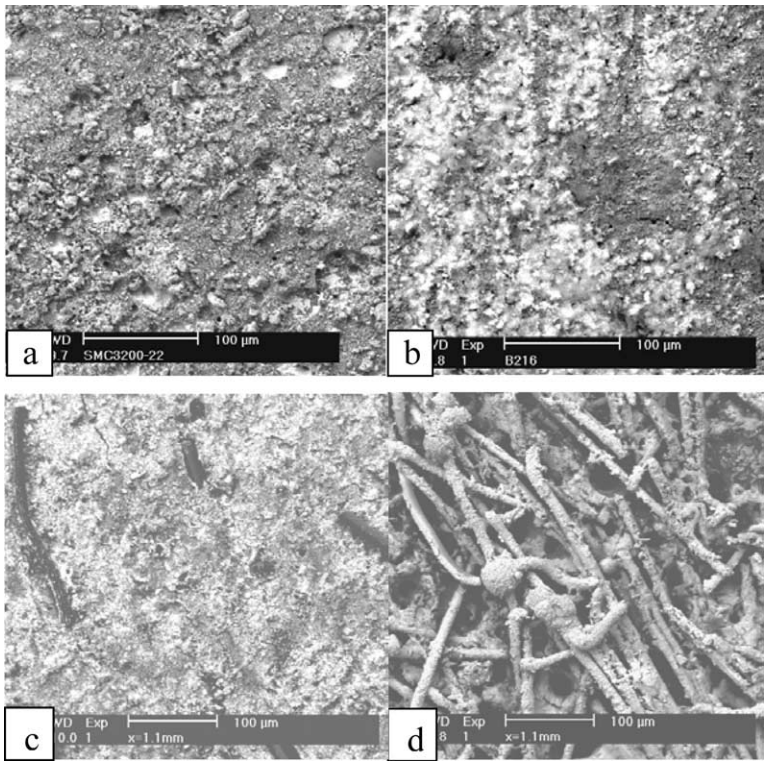

Fig. 1. Examples of SEM images of the surface morphology for different polymeric materials after arc exposure demonstrating non-uniformity on a large scale: polyester (a) and polyamide 66 (b) after five arc shots; glass-filled polyamide 66 far from (c) and close to (d) the arc zone.

interaction with arc and covered by large surface corrugations. Detailed characterization of these sub-micron changes cannot be easily revealed with traditional techniques and may be very important for the understanding of their dielectric breakdown performance under variable arc conditions under very initial stages of surface reorganization. However, the question of how surface morphology of different materials is altered during arc shots at a very small scale and at low current conditions frequently it is not even addressed. Changes of surface morphology at nanoscale can be critical for the understanding of dramatic changes in surface resistivity preceding electric breakthrough.

In this work, we exploit an atomic force microscopy (AFM) technique to obtain true 3D topography on a sub-micron scale after arc exposure with lower current for representative polymer composites typically used in low voltage power circuit breakers. We did not address the later stages of interactions accompanied by full coverage with carbonized material and metal deposits. We also did not consider the total surface changes at large scales occurring in the process, a question which was addressed in other studies [5]. We focused on quantification of the surface topography of polymers themselves on a sub-micron scale by evaluating the surface microroughness for these materials on a sub-micron area (less than $5\times5\ \mu m^2$ scanning size) not covered with large agglomerates of deposited material. The most dramatic changes can occur at very early stages of interactions between low-energy arc and the polymer surface resulting in dramatic decrease of the surface resistivity which compromise circuit breaker performance well before the visible and continuous carbonized/metallized surface layer is formed [9]. These, pre-catastrophic changes in surface conductivity could be caused by minor but important changes in surface morphology on a nanoscale preceding large-scale specimen alternations easily detectable with optical microscopy and SEM and discussed in detail in literature [5]. We observed changes of polymer surfaces with nanoscale resolution and suggested mechanisms of their initial reorganization through deposition and surface melting which are very different for different locations (in proximity to the arc origination zone and far from it) and for different types of polymers, highly-crosslinked thermosets and crystallizable thermoplasts.

Thus, for this study, two types of polymer composites were selected, laminated polyester and polyamide 66, representing very different and widely used classes of plastics for circuit breakers: glass reinforced thermoset and thermoplastic material, respectively. This selection allows us to address the question of influence of the fundamentally different behavior of polymers (ability to melt and solidify for thermoplast and highly crosslinked nature of thermoset material). Based on AFM data for nanoscale 3D surface morphology from these different plastics subjected to a variable number of electrical arc shots, we suggested a chain of events (ablation, deposition, and re-melting) which may

lead to the characteristic surface morphologies after expose to electrical arc and which differs significantly for two materials studied here.

2. Experimental section

2.1. Materials

Several sets of glass–fiber reinforced laminated polyesters (NEMA GPO-3 grade thermoset) and polyamide 66 sample (thermoplastic) were compared for their surface morphology before and after arc exposure. The laminated polyester sheet was produced by combining polyester resin with glass mat (about 13%) and other additives including aluminum trihydrate as a flame-retardant. This material exhibits high flame resistance and is widely used in breakers as arc stack side and back, blade shield, and support. Polyamide 66 studied here as a representative of thermoplastic materials is used in current-limiting breaker as an arc cheek. When exposed to the electrical arc, polyamide 66, a high ablative material, provides a flow of gas, which is directed toward the arc. The produced gas forces expansion of the arc, and helps cooling down and quenching the arc.

2.2. Experimental setup

The experimental setup was designed to approximate the volume of a small circuit breaker as described in detail elsewhere [10]. Basically, the power source was a capacitor bank discharge circuit providing half-cycle current up to 30 kA peak value. Polymer sidewalls were exposed to arcing once the mobile contact opened, and typical arc energy ranged between 5 and 11 kJ per a single shot. Another experimental setup was used for the second set of samples. Fig. 2 shows a schematic of this arc chamber arrangement for this setup with appropriate geometrical dimensions. In this design, current-carrying conductor parted away from the zero line to a maximum distance of 5 mm. The two mobile metal contacts were AgCdO 95/5.

2.3. Experimental procedure

2.3.1. First set of samples

Glass-filled laminated polyester and polyamide 66 samples were exposed to five consecutive electrical arc shots at 10.2 kA peak current each corresponding to a total energy of 25 kJ for each sample.

2.3.2. Second set of samples

We prepared additional set of samples with very modest arc exposure to investigate very initial stages of the deposit formation. These samples were all glass-filled laminated polyester and were given a fewer number of shots with lower energy. We selected 1, 2, 3 and 5 shots sequences with a peak current of 3.2 kA and the energy per shot of about 0.7 kJ which represented a very low energy as compared to the first set.

2.4. AFM measurements

AFM topographical and friction images were collected using Dimension 3000 AFM microscope (Digital Instruments) in the contact mode under ambient conditions in accordance with a usual procedure adapted in our laboratory [11–13]. Silicon V-shaped tips with spring constants of 0.35 N/m were used for most scans. Tip radii were in the range of 20–40 nm as calculated from the profiles of a reference gold nanoparticle standard [14]. AFM images were obtained on different scales ranging from 1 to 40 μm across with a usual scanning rate of 1 Hz. Samples were scanned along two lines on different distance from the arc zone: −12.5 and −25 mm as indicated in Fig. 2. Each of these lines was scanned at the center and at the edges and each of this spots was scanned three times at four different scales to get sufficient statistical data distribution. To obtain the rms microroughness, a 1×1 μm^2, 2×2 μm^2, 3.5×3.5 μm^2, and 5×5 μm^2 surface areas were scanned.

Scanning at larger surface areas was challenging due to a very rough surface morphology with peak-to-valley roughness exceeding the limits of the AFM cantilever scanning capability (up to 20 μm) thus, preventing us from random sampling of the surface morphology all over the sample

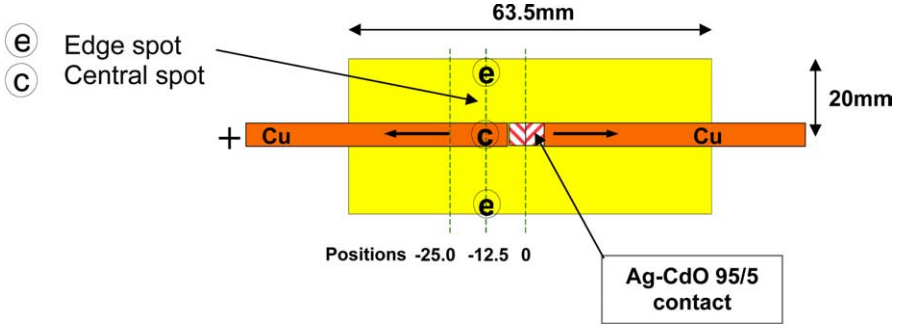

Fig. 2. Schematics of experimental setup for arc treatment and the selection of surface locations for morphology investigations.

areas and especially in the areas affected by large-scale depositions. Therefore, no detailed AFM studies and mechanism discussion were conducted for set 1 samples treated with high power electric arcs.

The results presented here were collected for set 2 samples treated with low power electric arcs (two orders of magnitude below that used for set 1). The AFM data analyzed here are representative for the fraction of the surface not affected by large-scale deposits which represents vast majority of surface area (>90% for set 2 specimens) except for the specimen treated with maximum (5) arc shots where the affected surface area reaches 20% for polyamide 66 and 50% for laminated polyester. Therefore, the results discussed here are representative surface sampling for all samples except one specimen of heavily treated polyester where they represent lower limit of surface alternation. For these specimens, the AFM data were representative and used for detailed analysis and suggestion of the mechanisms of the surface morphology alternation at earlier stages.

3. Results and discussion

Fig. 3 shows optical micrographs for both types of materials studied here (1st set of samples) before and after five consecutive arc shots at 10.2 kA corresponding to a total energy of 25 kJ. Both as-received specimens showed relatively uniform surface with highly developed texture caused by the molding process (Fig. 3(a) and (b)). After arc exposure, the polyamide surface looked uniformly re-melted with initial texture disappearing and some inclusions showing up as black randomly occurred dots (Fig. 3(c)). Unlike polyamide, the surface of laminated polyester after the arc treatment was covered by the extensive areas of black particles and aggregates (Fig. 3(d)).

As-received (not exposed to the arc) glass-filled laminate polyester and polyamide 66 samples were scanned for the initial evaluation of the surface morphology (Fig. 4(a) and (b)). As was observed, the surface of the polyester sample was covered with small particles (less than 300 nm in diameter) visible only at higher magnification. The original surface was relatively smooth and uniform even for larger scan sizes (Fig. 4(b)). When comparing these images with those obtained for polyamide 66 sample (Fig. 4(c) and (d)) it can be concluded that at the higher magnification the polyamide surface was less uniform and displayed higher microroughness than the polyester sample. This difference became even more evident for larger scan sizes because

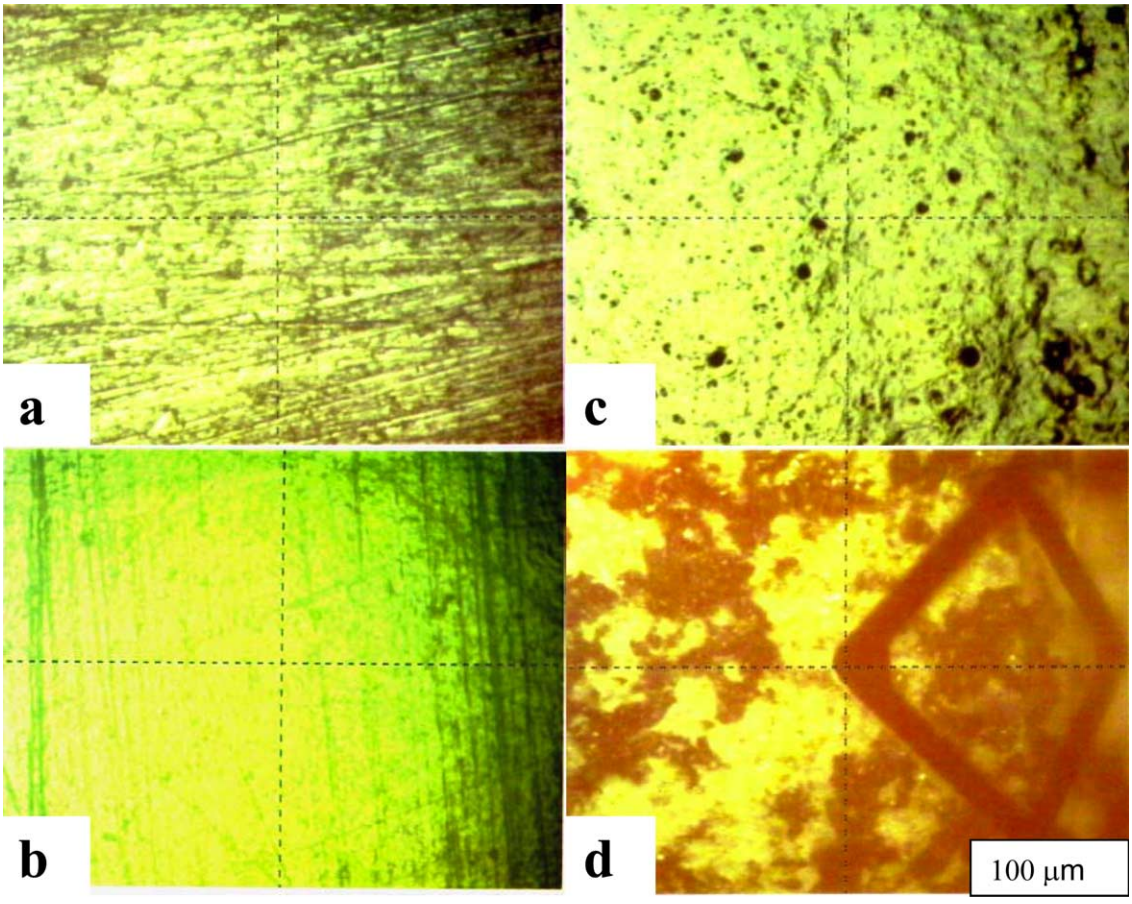

Fig. 3. Optical images of polymer composites before (a), (b) and after arc exposure ((c), (d), after five arc shots) for polyamide 66 (a), (c) and laminated polyester (b), (d). The V-shaped AFM tip demonstrates selection of the surface areas for scanning.

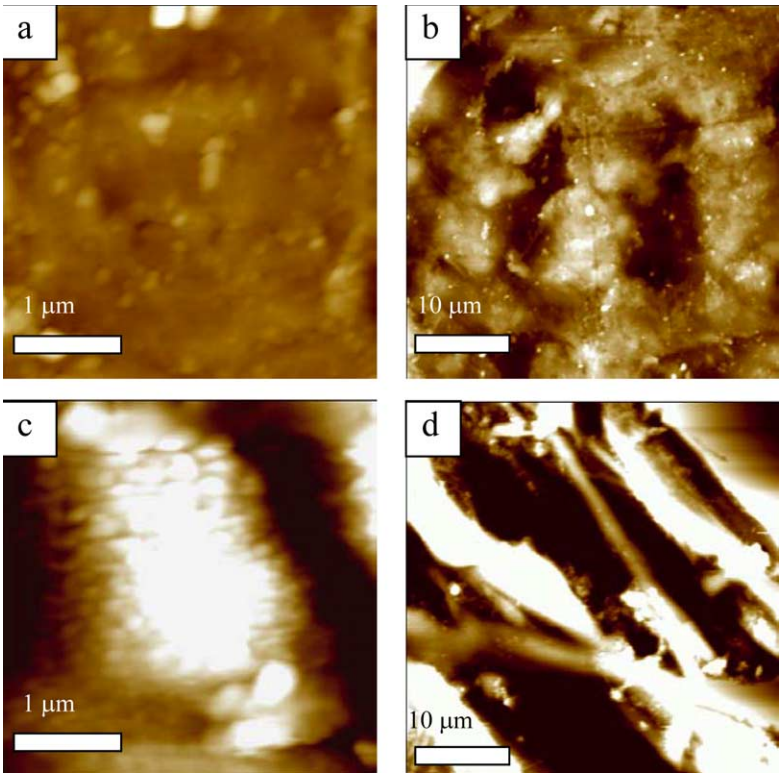

Fig. 4. AFM images of the surface morphology for as-received samples. (a), (b) High and low magnifications for laminated polyester; (c), (d) high and low magnifications for polyamide 66. *Z*-scale is 200 nm for the left column and 500 nm for the right column.

high ridges and deep grooves became visible in the selected surface areas (Fig. 4(d)).

Significant change of the initial surface morphology of both thermoset and thermoplastic materials was observed at the −12.5 mm line (close to arc origination zone) after applying five consecutive arc shots (Table 1). Microroughness data before and after arc shots (reference sample and treated sample) for polyester samples clearly showed an increase of the microroughness. For small scan sizes ($1\times 1\ \mu m^2$ and $2\times 2\ \mu m^2$), the value of the microroughness increased up to five times after the arc treatment. For larger scan sizes ($3.5\times 3.5\ \mu m^2$ and $5\times 5\ \mu m^2$), the microroughness increased up to 20 times as compared to the initial untreated samples. Contrary, the microroughness at different length scales for polyamide 66 consistently decreased after arc treatment by 2–8 times (Table 1). The microroughness recorded at the center and at the edges of these samples was very different for two sets of samples (see data in Table 1).

Such differences in the surface morphology for polyester and polyamide 66 materials after the arc treatment may be explained by inherently different thermal properties of these materials. After arc shots, the surface of polyamide sample (thermoplastic) was ablated and the new surface re-melted due to high temperature in the vicinity of the arc zone. As a result of the re-melting the initial non-uniform surface was smoothened during the cooling cycle and the overall surface microroughness decreased dramatically. In the case of the polyester specimen, the intensive ablation of the material from the arc origination zone should occur without any re-melting of the surrounding surface areas. Because these samples were exposed to five arc shots, their surface

Table 1
Microroughness data for glass-filled polyester laminate and polyamide 66 (PA 66) samples

Material	Interrupting current (kA)	Roughness −12.5 mm	Roughness −12.5 mm	Roughness −12.5 mm	Roughness −12.5 mm	Roughness −2.5 mm
Polyester	10.2	$1\times 1\ \mu m^2$	$2\times 2\ \mu m^2$	$3.5\times 3.5\ \mu m^2$	$5\times 5\ \mu m^2$	$20\times 20\ \mu m^2$
Center		21±17	102±21	239±82	320±120	N/A
Edge		26±24	81±13	222±66	343±62	N/A
As-received	0	5±1		14±1		85±2
PA 66	10.2	$1\times 1\ \mu m^2$	$2\times 2\ \mu m^2$	$3.5\times 3.5\ \mu m^2$	$5\times 5\ \mu m^2$	$20\times 20\ \mu m^2$
Center		12±6	13±1	14±1	22±4	109±17
Edge		5±2	7±2	10±2	14±2	147±50
As-received	0	5±1		81±3		220±16

morphology corresponded to the final stage of material treatment.

An additional set of glass-filled polyester laminate samples with a different number of arc shots discussed next was prepared by using experimental setup shown on Fig. 2 to determine surface morphology changes at very early stages of the interaction with electrical arc. In these cases, large surface deposition was minimal and AFM sampling was easily conducted on randomly selected areas without interference from large flakes. During the preparation of these samples, lower current (3.2 kA peak value) was used to make possible a detailed AFM investigation of the carbonization/metallization process at very early stage. All specimens were scanned at the −12.5 mm line and AFM images were taken at the center and at the edges of the sample. Fig. 5 shows high resolution AFM images of the polyester sample subjected to a different number of arc shots. Various features (bumps, grooves, and ridges) of the surface morphology were observed for different surface areas along the sample edge (Fig. 5, left column) and in the vicinity of the sample center (Fig. 5, right column). Along the edges, the density of small and medium-sized bumps that appeared after the first arc shot (Fig. 5(a), left column) decreased with the number of arc shots, and small bumps completely disappeared after the fifth arc shot (Fig. 5(c), left column).

At the center of sample, very different changes in the surface morphology were observed (Fig. 5, right column). After the first arc shot, few large (>0.1 μm) bumps became visible (Fig. 5(a), right column). With the increasing number of arc shots, these bumps were replaced by larger hills with the lateral size reaching 1 μm and the height of 500 nm or higher. The variation of the surface morphology at the edges and the center of the samples was quantified by measuring the surface microroughness for small and large scan sizes (Fig. 6). At the sample edges, the surface microroughness rapidly increased after a single arc shot. After following shorts, the surface morphology remained quite unchanged (similar microroughness values within a standard deviation range) for both small and large scan sizes (Fig. 6(a) and (c)). At the center of the samples, the surface microroughness rapidly increased after first arc shot and remained very large for surfaces after treatment with an increasing number of arc shots (Fig. 6(b) and (d)).

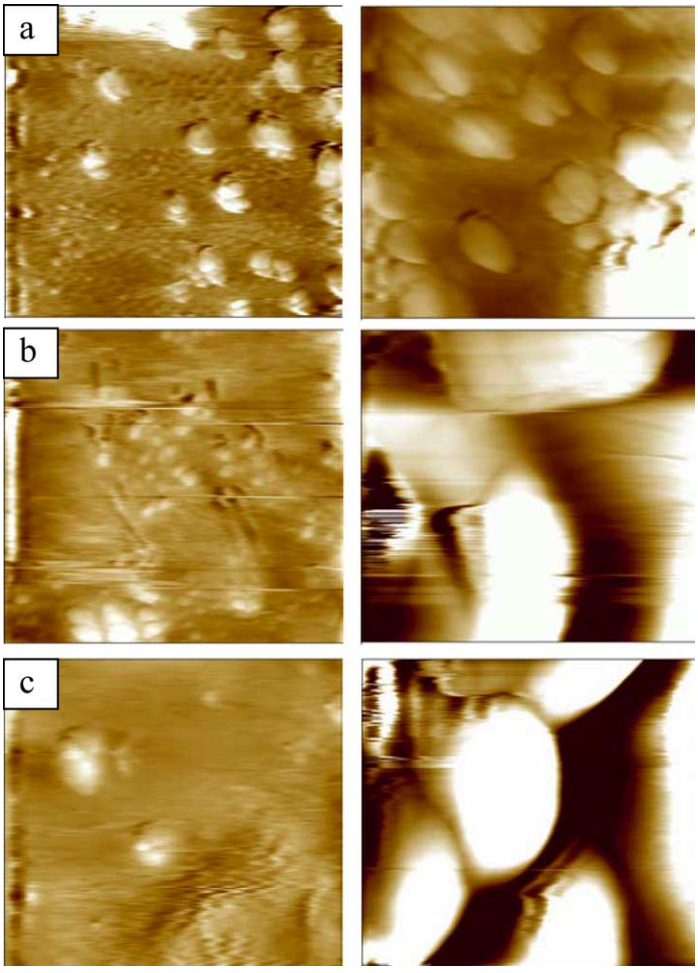

Fig. 5. AFM images (1×1 μm^2 size for all images) of laminated polyester at −12.5 mm line for the front location (left column) and the center location (right column) after (a) one arc shot; (b) three arc shots; (c) five arc shots. *Z*-scale is 200 nm for all images.

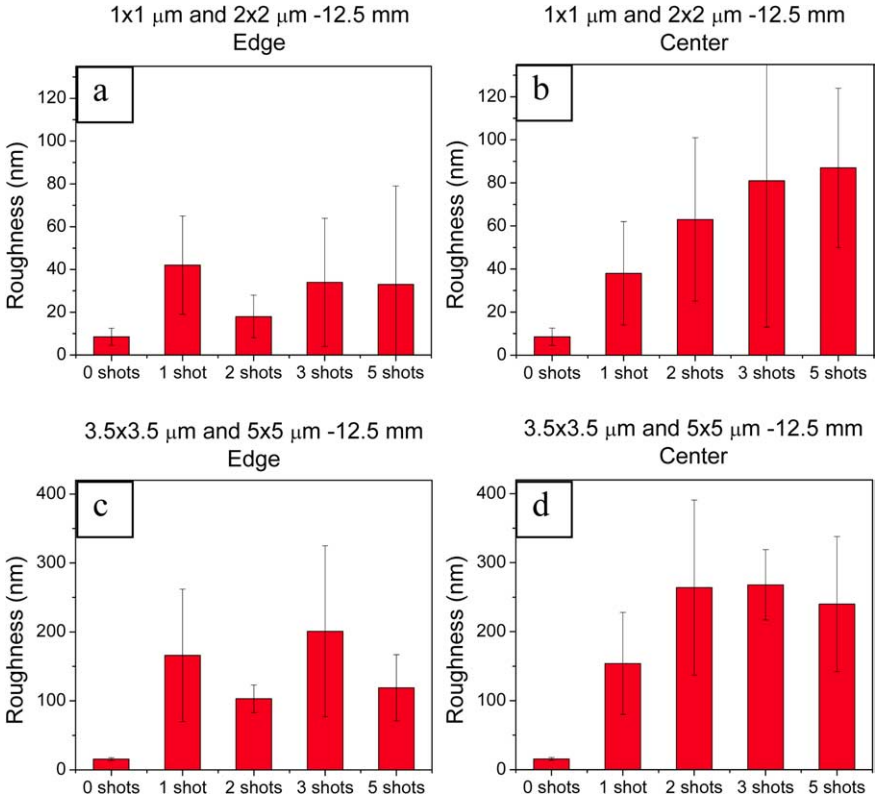

Fig. 6. The microroughness of the laminated polyester at the sample edge (left column) and at the center of the sample (right column) along −12.5 mm line. (a), (b) Combined data for surface areas below 2×2 μm^2; (c), (d) combined data for surface areas up to 5×5 μm^2.

Based on AFM images and the surface microroughness data for laminated polyester material, we proposed a scenario of events which describes the surface morphology variation at the center (close to arc formation zone) and along the edges of sample (Figs. 7 and 8) in the course of increasing number of arc shots. As known, an intense interaction of high-temperature plasma with polymer surfaces results in continuous ablation of the materials. As a consequence, the topmost material layer is pulled out of the surface near the arc origination zone and condenses along the edges (far from the arcing zone with rapidly decreasing temperature) of the samples. As a result of this re-deposition process, a lot of medium (100–200 nm in diameter) and small (less than 50 nm in diameter) particles became visible on the surface after the first arc shot (Fig. 7(a)). With the increasing number of arc shots, nanoparticles covered the surface densely demonstrating intense coalescence and aggregation and the deposition of additional particles. On the other hand, the average size of particles deposited at this stage increased to 200 nm (Fig. 7(b)). After five arc shots (Fig. 7(c)), the entire surface was completely and uniformly covered by deposits with only few large bumps still occasionally observed.

At the same time, at the center of laminated polyester sample (in the vicinity of the arc origination), large bumps and grooves appeared already after the first arc shot (Fig. 8(a)). This difference in the surface morphology can be associated with the intensive ablation process in the course of plasma etching leading to fast removal of relatively large (close to a micron) pieces of the topmost surface. During this process, the topmost material was non-uniformly pulled out with few larger microscopic bumps and grooves created as a result. These surface bumps were separated from each other by deep holes and grooves. With the increasing number of arc shots (three and five consecutive arc shots), the progressive ablation process apparently resulted in increasing heterogeneity of the treated surface with only very few large grooves and bumps left within the surface areas scanned (Fig. 8(b) and (c)).

Direct comparison of the microroughness data for laminated polyester and polyamide 66 shows very different scenarios of dramatic changes of the surface morphology as can be concluded from Fig. 9. In fact, only in the very center of this sample, in close proximity to the arc initiation zone, the surface microroughness increased significantly at a microscopic level indicating modest roughening caused by the intensive polymeric material removal during the ablation process. Far from this central area, the polymer surface after arc treatment became more uniform. At larger spatial scale, the polyamide 66 surface, in fact, became much smoother after the arc treatment disregarding a specific surface location and a level of the proximity to the arc zone. At all surface locations and spatial scales

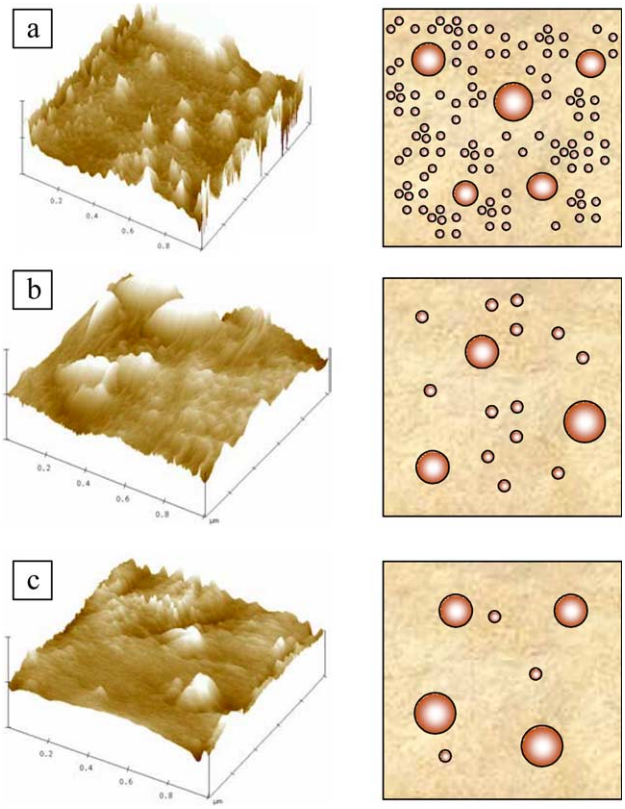

Fig. 7. Representative 3D AFM topographical images (left column) and corresponding sketches of the surface morphology (right column) for a different number of arc shots for laminated polyester along the sample edges: (a) 1 arc shot; (b) 3 arc shots; (c) five arc shots. *Z*-scale is 80 nm.

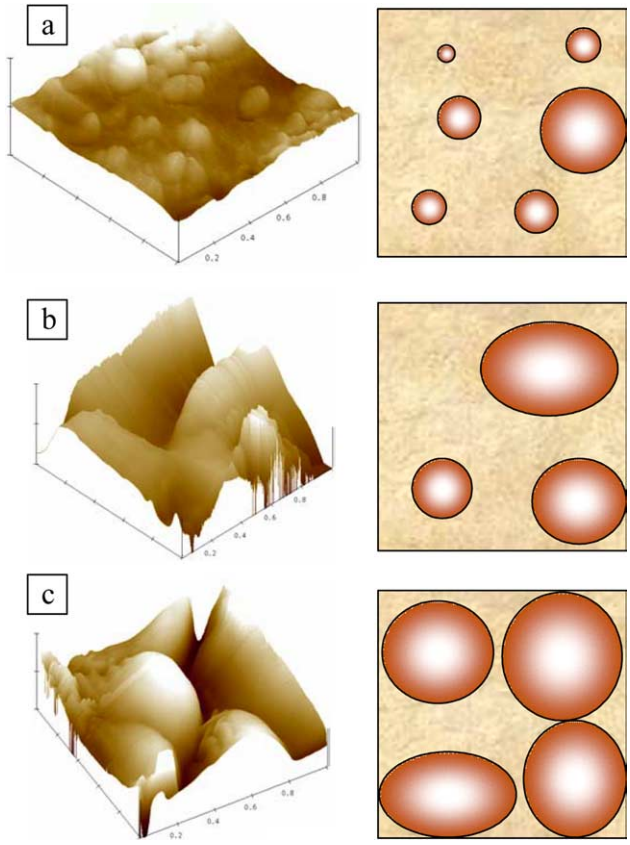

Fig. 8. Representative 3D AFM topographical images (left column) and corresponding sketches of the surface morphology (right column) for different number of arc shots for laminated polyester at the center: (a) one arc shot; (b) three arc shots; (c) five arc shots. *Z*-scale is 200 nm.

analyzed here, we observed progressive smoothening as indicated by 4–6 times decrease in the microroughness values, well above standard deviations (Fig. 9). Apparently, total re-melting of the thermoplastic surface due to the high temperature exposure caused overall smoothing of the treated surface by filling initial inhomogeneities caused by the material ablation. In addition, it was observed that deposited sub-micron particles were not strongly attached to the surface for thermoset but are embedded in the matrix of thermoplastic material.

4. Conclusions

In conclusion, we tested representatives of thermoset, glass-filled laminated polyester, and thermoplastic, polyamide 66, materials and their behavior upon interaction with intense electrical arc. The main focus of this work was on very earlier stages of the surface reorganization under relatively few arc shots and on a very fine scale which is well below traditional scale of large scale aggregates and deposits formed on later stages of the polymer material degradation.

At these early stages and at nanoscale spatial scale, we observed that arc exposure resulted in the significant increase of the surface microroughness for the surface areas in close proximity to the arc zone initiation for both materials studied here (thermoplast and thermoset). This change was caused by the appearance of sub-micro- (100–1000 nm) and nano- (<50 nm) particles on the polymer surface. For thermoset material, the initial deposition of nano- and micro-particles along the sample edges at the earlier stages was followed by gradual surface smoothing for the increasing number of arc shots. The central area under the arc zone became increasingly heterogeneous with prolonged treatment due to more intensive ablation and heterogeneous removal of the material. On the other hand, the surface areas far from the center and close to the edges of the samples became much smoother due to the preferential deposition of a thin surface layer of the carbonized material far from the arc initiation zone.

Different physical properties of two materials studied here are critical for very different surface reorganization observed here. We suggest that for highly-crosslinked laminated polyester, intense electric arc results in the ablation of the polymer material without local surface melting. The material is carbonized and pulled out of the surface in the form of micron-size particles in the vicinity of the arc initiation zone with maximum electric field (the

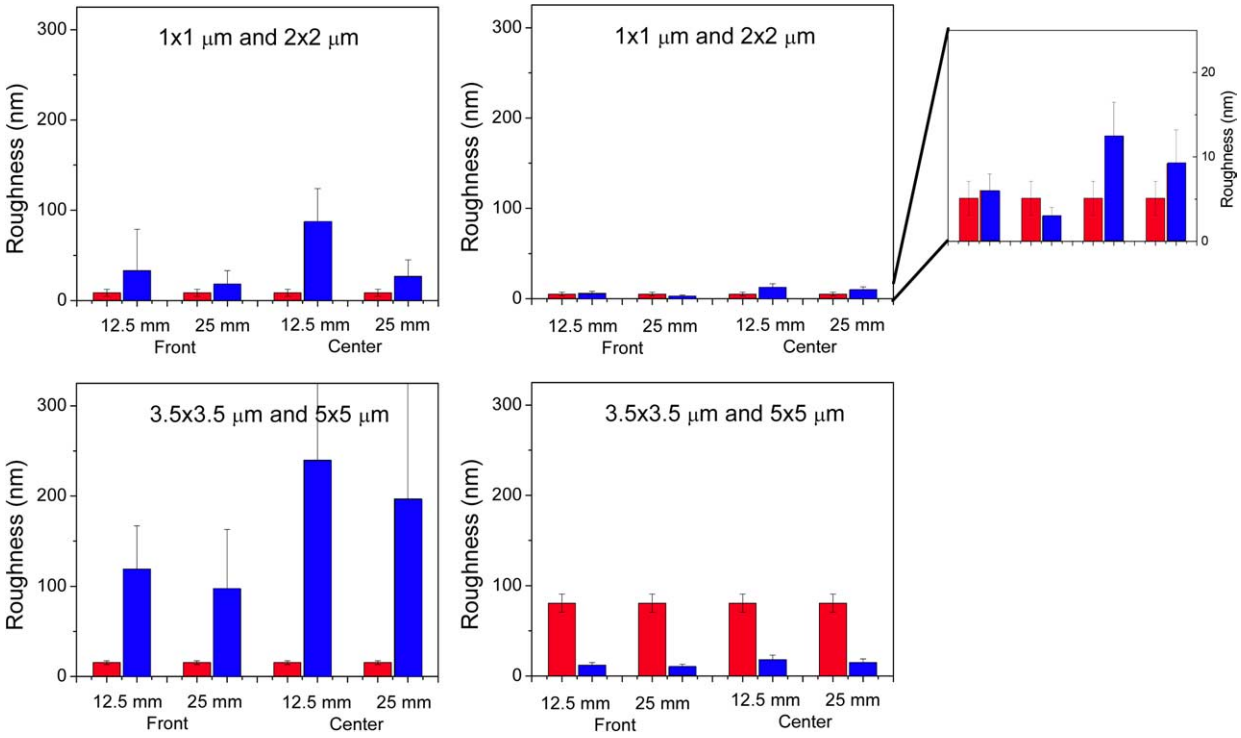

Fig. 9. Summary plots for the microroughness of the laminated polyester (left panels) and polyamide 66 (right panels) for the surface areas smaller than $2\times 2\ \mu m^2$ (top) and for the surface areas up to $5\times 5\ \mu m^2$ (bottom) for different numbers of shots and different locations. Left column is for the original surface; right column is after five shots. Insert shows an enlarged scale for polyamide 66.

center of the sample) due to heterogeneous thermal degradation of the surface layer due to intense thermally initiated scission of the polymer network. Intensive re-deposition of these particles occurs far from the arc zone and along the edges with lower temperature enhancing non-uniform surface morphology. Whereas, under similar conditions, the thermoplastic polyamide material behaves very differently. High temperature in the central area close to the arc zone causes intense melting and evaporation of the polyamide material preventing ablation of large particulate material. The evaporazed/carbonized material is re-deposited along the edges with reduced temperature resulting in melting followed by solidification of the polymer surface all over the specimen. This different chain of events leads to the overall surface smoothing and more uniform surface coverage by the re-melted material for polyamide material. Therefore, very different initial properties of polymeric materials, highly crosslinked polyester and crystallizable polyamide, cause very different process of their degradation in the course of interaction with intense electric arc, resulting either in highly heterogeneous microscopic morphology in the former case and in highly smoothened morphology in the latter case. The difference revealed here could causes very different changes in surface resistivity associated with the level of carbonization and metallization of the affected surfaces as will be a subject of forthcoming studies.

Acknowledgements

The authors would like to thank J.L. Ponthenier, Schneider Electric, Grenoble for providing test materials, information, and SEM images, and Square D/Schneider Electric for the financial support.

References

[1] Kovitya P. IEEE Trans Plasma Sci 1984;PS-12:38.
[2] Slade PG, editor. Electrical contacts principles and applications. New York: Marcel Dekker; 1999. p. 476.
[3] Chevrier P, Barrault M, Fievet C, Maftoul J, Fremillon JM. J Phys D: Appl Phys 1997;30:1346.
[4] Fievet C, Barrault M, Petit P, Chevrier P, Fleurier C, Andre V. J Phys D: Appl Phys 1997;30:2991.
[5] Ponthenier JL, Laverty F, Teulet P, Mercado-Cabrera A, Gleizes A. E-MRS 2004 Spring Meeting, Strasbourg, France; 2004. To be published.
[6] Shea JJ. IEEE Trans Electrical Contact 2000;46:161.
[7] Shea JJ. IEEE Trans Electrical Contact 2002;48:70.
[8] Ponthenier JL. Private communication.
[9] Rapeaux M. Unpublished results.
[10] Fievet C, Chevrier P, Fleurier C, Andre V, Gleizes A. 14th ISPC, Prague, Czech Republic; 1999. p. 657.
[11] Tsukruk VV, Reneker DH. Polymer 1995;36:1791.
[12] Tsukruk VV. Rubber Chem Technol 1997;70:430.
[13] Ratner B, Tsukruk VV, editors. Scanning probe microscopy of polymers. ACS symposium series, vol. 694.
[14] Vesenka J, Manne S, Giberson R, Marsh T, Henderson E. Biophysical J 1993;65:992.